The European Physical Journal E

Synchrotron X-ray Study of Intrinsically Disordered and Pollyampholytic Tau 4RS and 4RL under Controlled Ionic Strength

--Manuscript Draft--

Manuscript Number:	EPJE-D-23-00143R1
Full Title:	Synchrotron X-ray Study of Intrinsically Disordered and Pollyampholytic Tau 4RS and 4RL under Controlled Ionic Strength
Article Type:	Reply to Comment
Manuscript Classifications:	100: I. Soft Matter; 100.010: Polymers and Polyelectrolytes
Section/Category:	Experimental
Funding Information:	KAIST (KAIST KC30-N11230021) — Professor Myung Chul Choi National Research Foundation of Korea (NRF-2021R1A6A3A13046235) — Ph.D. student Hasaeam Cho Korea Health Industry Development Institute (KHID/KDRC-MOHW/MIST-HU23C0094) — Professor Myung Chul Choi Korea Basic Science Institute (KBSI-MOE-2021R1A6C103B422) — Professor Myung Chul Choi National Research Foundation of Korea (NRF-MIST-2020M3A7B6026565) — Professor Myung Chul Choi National Research Foundation of Korea (NRF-2020R1F1A1054849) — Dr. Kyeong Sik Jin U.S. Department of Energy (DE-FG02-06ER46314) — Professor Cyrus R. Safinya National Science Foundation (DMR-1807327) — Professor Cyrus R. Safinya University of California, Santa Barbara (UCSB Academic Senate) — Professor Stuart C. Feinstein
Abstract:	Aggregated and hyperphosphorylated tau is one of the pathological hallmarks of Alzheimer's disease. Tau is a polyampholytic and intrinsically disordered protein (IDP). In this paper, we present for the first time experimental results on the ionic strength dependence of the radius of gyration (Rg) of human Tau 4RS and 4RL isoforms. Synchrotron X-ray scattering revealed that 4RS Rg is regulated from 65.4 to 58.4 Å and 4RL Rg is regulated from 70.9 to 57.8 Å by varying ionic strength from 0.01 to 0.59 M. The Rg of 4RL Tau is larger than 4RS at lower ionic strength. This result provides an insight into the ion-responsive nature of intrinsically disordered and polyampholytic Tau, and can be implicated to the further study of Tau-Tau and Tau-tubulin intermolecular structure in ionic environments.
Corresponding Author:	Myung Chul Choi, Ph.D KAIST: Korea Advanced Institute of Science and Technology Deajeon, KOREA, REPUBLIC OF
Corresponding Author Secondary Information:	
Corresponding Author's Institution:	KAIST: Korea Advanced Institute of Science and Technology
Corresponding Author's Secondary Institution:	
First Author:	Hasaeam Cho
First Author Secondary Information:	
Order of Authors:	Hasaeam Cho Jimin Lee Hanjoon Nho

	Keunmin Lee
	Bopil Gim, Ph.D.
	Juncheol Lee, Ph.D.
	Jaehee Lee
	Kai K. Ewert, Ph.D.
	Youli Li
	Stuart C. Feinstein, Ph.D.
	Cyrus R. Safinya, Ph.D.
	Kyeong Sik Jin, Ph.D.
	Myung Chul Choi, Ph.D.
Order of Authors Secondary Information:	
Author Comments:	
Response to Reviewers:	
Suggested Reviewers:	Gerard Wong, Ph.D. Professor, UCLA: University of California Los Angeles gclwong.ucla@gmail.com X-ray scattering study of Soft Matter and Biological System
	Tim Salditt, Ph.D. Professor, University of Gottingen: Georg-August-Universitat Gottingen tsaldit@gwdg.de X-ray scattering of Soft Matter and Biological Systems
	Kwanwoo Shin, Ph.D. Professor, Sogang University kwshin@sogang.ac.kr X-ray scattering of Soft Matter and Biological Systems

Synchrotron X-ray Study of Intrinsically Disordered and Polyampholytic Tau 4RS and 4RL under Controlled Ionic Strength

Hasaeam Cho[1], Jimin Lee[1], Hanjoon Nho[1], Keunmin Lee[1], Bopil Gim[1], Juncheol Lee[1], Jaehee Lee[1], Kai K. Ewert[2], Youli Li[3], Stuart C. Feinstein[4], Cyrus R. Safinya[2], Kyeong Sik Jin[5,6], Myung Chul Choi[1*]

[1]Department of Bio and Brain Engineering, KAIST, Daejeon 305-701, Korea*
[2]Materials Department, Molecular, Cellular, and Developmental Biology Department, Physics Department, and Biomolecular Science and Engineering Program, University of California, Santa Barbara, California 93106, USA
[3]Materials Research Laboratory, University of California, Santa Barbara, California 93106, USA
[4]Neuroscience Research Institute, Molecular, Cellular, and Developmental Biology Department, and College of Creative Studies Biology, University of California, Santa Barbara, California 93106, USA
[5]Pohang Accelerator Laboratory, POSTECH, Pohang 37673, Korea
[6]Division of Advanced Nuclear Engineering, POSTECH, Pohang 37673, Korea

*Corresponding author. E-mail: mcchoi@kaist.ac.kr

Abstract. Aggregated and hyperphosphorylated tau is one of the pathological hallmarks of Alzheimer's disease. Tau is a polyampholytic and intrinsically disordered protein (IDP). In this paper, we present for the first time experimental results on the ionic strength dependence of the radius of gyration (R_g) of human Tau 4RS and 4RL isoforms. Synchrotron X-ray scattering revealed that 4RS R_g is regulated from 65.4 to 58.4 Å and 4RL R_g is regulated from 70.9 to 57.8 Å by varying ionic strength from 0.01 to 0.59 M. The R_g of 4RL Tau is larger than 4RS at lower ionic strength. This result provides an insight into the ion-responsive nature of intrinsically disordered and polyampholytic Tau, and can be implicated to the further study of Tau-Tau and Tau-tubulin intermolecular structure in ionic environments.

Keywords: Tau, IDP, R_g, X-ray scattering

1 Introduction

The protein Tau is mostly localized in axons of neurons and plays a key role in neuronal development including cell polarity, outgrowth, dendrite pruning, and DNA protection. [1-8] Tau is known as a microtubule-associated protein (MAP). Tau binds to microtubule (MT), regulates tubulin assembly, and stabilizes MTs. [9-12] Aberrant Tau behavior is correlated with numerous neurodegenerative diseases including Alzheimer's,

Pick's, supranuclear palsy, and fronto-temporal dementia with Parkinsonism linked to chromosome 17 (FTDP-17) [13, 14].

Tau is an intrinsically disordered protein (IDP) that lacks a secondary structure in solution. [15, 16] In cells, Tau undergoes liquid-liquid phase separation (LLPS) similar to several IDPs and low-complexity regions in proteins, with high local protein concentration within condensed drops. [17, 18] The Tau structure is often described sequentially from the N- to the C-terminus: human wild-type Tau 4RS and 4RL possess four imperfect repeats (R1, R2, R3, and R4) and differ in the N-terminal region by possessing either zero or two sections of 29 amino acids, thereby generating short (S-) or long (L-) isoforms. Tau is a polyampholyte that contains both positive and negative charges within a single Tau. The MT binding domain is rich in positive charge and the N-terminal tail contains regions of negative charge as well as regions rich in positive charge (**Fig. 1B**). Tau is overall cationic with charge in a range of 5.9 – 16.5 *e* at pH 6.8. [9-12]

This intrinsically disordered and polyampholytic nature makes it difficult to understand the structure and function of Tau. The radius of gyration (R_g) a size parameter (or mass distribution) is defined as the square root of the average squared distance of each scatterer from the particle center. [19] The R_g of 4RL Tau (2N4R or ht40) was measured to be on average 6.5 – 7 nm at room temperature and 5.5 – 7 nm at various temperatures (280 – 333 K). [20-24] Molecular dynamics (MD) simulations gave an R_g of 6.53 nm for 4RL. [25]. For 3RS (0N3R or ht23) and 3RL (2N3R) Tau, R_g values were measured to be 5.3 nm and 6.33 nm, respectively. [20, 21, 24]

Tau is abundant in charged residues and the ionic strength of its solution can be attributed to the conformational transition, which minimizes or maximizes the electrostatic interaction. [26, 27] Human 4RL Tau fibrillation into paired helical filaments (PHFs) found in the brains of AD patients can be induced by heparin, and decreases with increasing ionic strength. [26, 27] In condensed LLPS drops, PHF formation is promoted in the presence of heparin, and is dependent on ionic strength: PHFs were not observed at NaCl concentrations of 200 mM and above. In the absence of heparin, however, Tau MTBRs merely form PHF despite ionic strength changes in 0-300 mM NaCl. [17] Tau LLPS formation is sensitive to the salt concentration, being enhanced at low salt concentrations and inhibited at high concentrations by adding more than 200 mM NaCl or KCl. [18, 28] X-ray scattering can be employed to quantitatively characterize the overall structure and structural transitions of partially or completely unfolded proteins and metastable objects. [21] However, the overall size of Tau protein under ionic strength regulation is not yet understood, and remains to be elucidated.

In this paper, we have used synchrotron X-ray scattering to investigate the structure (i.e. R_g) of human Tau 4RS and 4RL isoforms under controlled ionic strength. We show that the R_g value of both 4RS and 4RL Tau are regulated with varying ionic strength in the range of 0.01 – 0.59 M.

2 Materials, Method, and Results

2.1 Tau protein preparation

Tau is expressed in BL21 (DE3) competent cells. After incubation in LB and auto-induction media (10 g of tryptone, 5 g of yeast extract, 0.5 g of dextrose, 2 g of α-D-lactose and 5 mL of glycerol per liter of 25 mM Na_2HPO_4, 25 mM KH_2PO_4, 50 mM NH_4Cl, 5 mM Na_2SO_4, and 4 mM $MgSO_4$ in DI water) for 24 h, cells were collected via centrifugation, and were re-suspended in BRB80 (80 mM PIPES/NaOH at pH 6.8, 1 mM EGTA, 1 mM $MgSO_4$), [9-12] lysed via sonication, and then subsequently boiled and centrifuged again. The supernatant was run through a phosphocellulose (P11 Whatman) anionic exchange column, with Tau binding to the phosphocellulose, and eluted with increasing concentration of NaCl in BRB80. Fractions with Tau were buffer-exchanged into pure BRB80 via Amicon Ultra-15 Centrifugal Units (Millipore). Tau was loaded into a HiTrap hydrophobic interaction chromatography column (GE), and eluted with decreasing the concentration of $(NH_4)_2SO_4$ in BRB80. Tau was concentrated and the buffer was exchanged with pure BRB80 through successive centrifugation cycles using Amicon Centrifugal Units. The concentration of Tau stock was determined by SDS-PAGE comparison with a Tau mass standard (originally measured via amino acid analysis).

2.2 Control in ionic strength

For BRB80 buffer, [Pipes] = 80 mM, $[Pipes^{2-}] = [Pipes^{-}] \approx 40$ mM and $[Na^{+}] = [NaOH] = [Pipes^{-}] + 2 \times [Pipes^{2-}] \approx 120$ mM, at pH ≈ 6.8 due to pKa_1=3.3 and pKa_2 = 6.85 at 20 °C. [29] The ionic strength, $\mu = \Sigma\, \rho_i z_i^2 / 2 = ([Pipes^{2-}] \times (-2)^2 + [Pipes^{-}] \times (-1)^2 + [Na^{+}] \times (+1)^2) / 2 = ([0.04] \times (-2)^2 + [0.04] \times (-1)^2 + [0.12] \times (+1)^2) / 2 = 0.16$ M. (With $[MgCl_2]$ = 1 mM, and [EGTA] = 1 mM, μ ≈ 0.165 M, while EGTA is a chelator of Mg^{2+} ion.) To vary the ionic strengths at constant pH: PEM80 buffer was diluted by adding deionized water, thus μ = 0.01 – 0.165 M. KCl was added to PEM80 buffer for μ = 0.165 – 0.59 M. [9, 30-31]

2.3 Synchrotron X-ray scattering.

Synchrotron X-ray scattering was carried out at the Pohang Accelerator Laboratory (PAL) beam-line 4C at 10 keV. [32] Scattering data were collected with a Rayonix 2D SX165 detector. Sample-to-detector distance was set to 4 m for SAXS or 4 m and 2 m for merging of SAXS and WAXS and calibrated with a silver behenate reference sample. The images were azimuthally averaged to obtain scattering intensity versus momentum transfer q. Fig. 2 shows a customized solution X-ray scattering cell: it is made of brass. A 1.5 mm quartz capillary was mounted in the cell. The temperature was controlled using an oil circulator (FP5-HE and H10, Julabo). Our scattering experiment was carried out at 20 ºC. As a control sample, bovine serum albumin (BSA) was loaded and data was compared with the known scattering patterns. Buffer data was previously collected for 10 sec as the background. For each scattering sample, data was collected for 10 sec which is the time for the Tau sample to be safe from radiation damage (see **Fig. S2**. Six rounds of data collection were averaged, and background buffer data was subtracted with PRIMUS. [33] The forward scattering *I(0)* and the radius of gyration

R_g were evaluated using the Guinier approximation, which states that the intensity can be represented as $I(q) = I(0)$ exp $[-(q^2R_g^2)/3]$ at small angles of $q < 1.3/R_g$. [19-20]

Tau samples for X-ray scattering were concentrated with an Amicon Ultra-0.5 device (Millipore) at 13170 g (RCF) for 10 min at room temperature. The final Tau concentration was 4 – 8 mg/mL. At least 25 μL of the sample was loaded in a 1.5 mm quartz capillary that had been washed with ethanol and deionized water.

Our X-ray samples used for the determination of R_g exhibits a completely linear Guinier plot (**Fig. S1**) indicating non-aggregated ones, which is distinguished from the aggregated sample of a nonlinear X-ray scattering profile at the small angle (q). Consistently, the gel permeation chromatography (GPC) result shown in **Fig. S3** has a single peak for 4RS Tau and no sign of aggregation.

Fig. 3(C-D) shows the azimuthally-averaged synchrotron X-ray scattering data of 4RS and 4RL with varying ionic strength $\mu = 0.01 – 0.59$. To quantitatively assess the effect of ionic strength on the R_g of Tau, the Guinier plots of scattering intensity vs. q^2 are shown in **Fig. 3(E-F)**, where the y-axis is in the log scale. Note that all the scattering data in the Guinier regime are linear, indicating that the Tau samples were not aggregated. **Fig. 3(G-H)** shows Kratky plots of $q^2I(q)$ *vs* q, which show featureless curves without apparent peaks which is typical for unfolded proteins. [20]

The fit of the X-ray data to the equation $I = I(0)\exp(-q^2R_g^2/3)$ gives the R_g of Tau. **Fig. 4** shows that the R_g of both 4RS and 4RL increases as the ionic strength (μ) decreases. With decreasing μ from 0.59 to 0.01 M, the R_g of 4RS Tau increases from 58.5 to 65.4 Å (12.0 % increase); R_g increases from 57.9 to 70.9 Å (22.7 % increase) for 4RL Tau. We note that the main change in R_g occurs at low ionic strength: For example, at $\mu \leq 0.165$, 76.4 % of the change in R_g occurs for 4RS and 77.0 % of the change for 4RL. The change in R_g then mostly saturates at $\mu > 0.165$. In comparison between 4RS and 4RL, 4RL is in general larger than 4RS. Particularly at $\mu = 0.01 – 0.083$, the difference in R_g between 4RS and 4RL is significantly large to be 5.37 ± 0.87 Å, but $\mu \geq 0.165$, the R_g of 4RL Tau is slightly larger ($\mu = 0.165 – 0.273$) and smaller ($\mu = 0.381 – 0.592$) than 4RS.

The R_g of unstructured protein is found to fit with Flory equation [34] $R_g = (1.927)N^{0.588}$ Å: $R_g = 69.15$ Å for 4RL ($N_{4RL} = 441$) and $R_g = 63.65$ Å for 4RS ($N_{4RS} = 383$). Our X-ray scattering data for the ionic strength $\mu = 0.083$ (Debye length is $1/\kappa = 10.59$ Å) which are $R_g = 62.05$ Å for 4RS and 66.48 Å for 4RL, are comparable to the theoretical estimation. On the other hand, at higher ionic strength $\mu \geq 0.165$ M, the smaller R_g with monotonically decreasing and isoform-independent manner might be due to the suppression of electrostatic interaction, thus the predominantly hydrophobic inter-residue attraction of single Tau. However, the structure and interaction of Tau isoforms for the low ionic regime have not been well understood yet, which needs to be elucidated.

3 Conclusion

We present a synchrotron solution X-ray scattering study to quantitatively measure the radius of gyration R_g of human Tau particularly the 4RS and 4RL isoforms in an ionic environment. Upon varying ionic strength from 0.01 – 0.59 M, R_g of Tau was

regulated: for 4RS, R_g increased from 58.4 to 65.4 Å; for 4RL R_g increased from 57.8 to 70.9 Å. Thus, 4RL Tau R_g is larger in a lower ionic strength environment than 4RS. This is the first experimental demonstration that the ionic strength dependence of the radius of gyration of full-length human Tau has been measured.

This paper provides insight into the regulation of the ionic environment-responsive nature of the intrinsically disordered and polyampholytic protein Tau. Changes in the charge environment such as a fluctuation in ionic strength or charge modification (e.g. post-translational modification including phosphorylation, etc.) might have significant effects on the structure and interaction of Tau and microtubules. [26-27, 35-36] For example, the expanded Tau molecules can be reactive to bind with another Tau or with tubulin in the neuronal cell. This highly interactive environment of Tau is analogously found in the confined space of Tau LLPS, where Tau-induced microtubule growth is known to occur. [18]

This result can be implicated to the further study of Tau-Tau and Tau-tubulin intermolecular structure regulated by the ionic environment. Molecular dynamics simulation study can determine the R_g of ionically regulated polyampholytic Tau.

Acknowledgments. This work was supported by KAIST KC30-N11230021, NRF-2021R1A6A3A13046235, KHID/KDRC-MOHW/MIST-HU23C0094, KBSI-MOE-2021R1A6C103B422 and NRF-MIST-2020M3A7B6026565. K.S.J. was supported by NRF- 2020R1F1A1054849. C.R.S., Y.L., and K.K.E. were supported by the US DOE, Office of Basic Energy Sciences, Division of Materials Sciences and Engineering under award number DE-FG02-06ER46314 (self- and directed assembly in charged biomolecular materials). Partial support was further provided to C.R.S. by the US NSF under award number DMR-1807327 (for protein phase behavior studies). S.C.F. was supported by a grant from UCSB Academic Senate.

Author contributions. The experiments were conducted by J.L., H.C., J.L., J.L., and K.J. The data were analyzed and discussed by J.L., H.C., C.R.S., Y.L., K.K.E, S.C.F., H.N., K.L., B.G., and M.C.C. The manuscript was written by H.C. and M.C.C. and reviewed by all authors.

Data availability. The data supporting this study are available from the corresponding author on reasonable request.

References

1. Scholz T. *et al.* Transport and diffusion of tau protein in neurons. *Cell. Mol. Life Sci.* **71**, 3139-3150 (2014).
2. Drubin D.G. *et al.* Nerve growth factor-induced neurite outgrowth in PC12 cells involves the coordinate induction of microtubule assembly and assembly-promoting factors. *J Cell Biol* **101**, 1799 –1807 (1985).
3. Esmaeli-Azad B. *et al.* Sense and antisense transfection analysis of tau function—tau influences net microtubule assembly, neurite outgrowth, and neuritic stability. *J Cell Sci* **107**, 869–879 (1994).

4. Ferreira A. *et al.* Microtubule formation and neurite growth in cerebellar macroneurons which develop in vitro: evidence for the involvement of the microtubule-associated proteins, MAP-1a, HMW-MAP2, and Tau. *Brain Res Dev Brain Res* **49**, 215–228 (1989).
5. Kempf M. *et al.* Tau binds to the distal axon early in development of polarity in a microtubule- and microfilament-dependent manner. *J. Neurosci.* **16**(18), 5583–5592 5591 (1996).
6. Herzmann S. *et al.* PAR-1 promotes microtubule breakdown during dendrite pruning in Drosophila. *EMBO J.* **36**, 1981–1991 (2017).
7. Rumpf S. *et al.* Functions of microtubule disassembly during neurite pruning. *Trends in Cell Biology* **29**(4), 291-297 (2019).
8. Sultan A. *et al.* Nuclear tau, a key player in neuronal DNA protection. *J. Biol. Chem.* **286**(6), 4566-4575 (2011).
9. Choi M. C. *et al.* Human microtubule-associated-protein tau regulates the number of protofilaments in microtubules: a synchrotron X-ray scattering study. *Biophys. J.* **97**, 519–527 (2009).
10. Chung P. J. *et al.* Direct force measurements reveal protein Tau confers short-range attractions and isoform-dependent steric stabilization to microtubules. *Proc. Natl Acad. Sci. USA* **112**, E6416–E6425 (2015).
11. Chung P. J. *et al.* Tau mediates microtubule bundle architectures mimicking fascicles of microtubules found in the axon initial segment. *Nat. Commun.* **7**, 12278-12286 (2016).
12. Choi M. C. *et al.* Paclitaxel suppresses Tau-mediated microtubule bundling in a concentration-dependent manner. *Biochimica et Biophysica Acta (BBA) – General Subjects* **1861**(1A), 3456-3463 (2017).
13. Kosik, K. S. *et al.* Microtubule-associated protein tau (tau) is a major antigenic component of paired helical filaments in Alzheimer disease. *Proc. Natl Acad. Sci. USA* **83**, 4044–4048 (1986).
14. Hutton, M. *et al.* Association of missense and 5'-splice-site mutations in tau with the inherited dementia FTDP-17. *Nature* **393**, 702–705 (1998).
15. Jeganathan S. *et al.* The natively unfolded character of tau and its aggregation to Alzheimer-like paired helical filaments. *Biochemistry* **47**, 10526–10539 (2008).
16. Skrabana R. *et al.* Intrinsically disordered proteins in the neurodegenerative processes: formation of tau protein paired helical filaments and their analysis. *Cellular and Molecular Neurobiology* **26**, 1083–1095 (2006).
17. Ambadipudi S. *et al.* Liquid-liquid phase separation of the microtubule-binding repeats of the Alzheimer-related protein Tau. *Nat Commun.* **8**, 275-287 (2017).
18. Hernández-Vega A. *et al.* Local nucleation of microtubule bundles through tubulin concentration into a condensed tau phase. *Cell Reports* **20**, 2304-2312 (2017).
19. Putnam C. D. *et al.* X-ray solution scattering (SAXS) combined with crystallography and computation: defining accurate macromolecular structures, conformations and assemblies in solution. *Quarterly Reviews of Biophysics* **40**(3), 191-285 (2007).
20. Mylonas E. *et al.* Domain conformation of tau protein studied by solution small-angle X-ray scattering. *Biochemistry* **47**, 10345–10353 (2008).
21. Shkumatov A. V. *et al.* Structural Memory of Natively Unfolded Tau Protein Detected by Small-Angle X-ray Scattering. Proteins 79, 2122−2131 (2011).
22. Bianconi A. *et al.* Temperature and solvent dependence of the dynamical landscape of tau protein conformations. *J Biol Phys* **38**, 169-179 (2012)
23. Battisti A. *et al.* Thermal compaction of the intrinsically disordered protein tau: entropic, structural, and hydrophobic factors. *Phys. Chem. Chem. Phys.* **19**, 8435 (2017).
24. Lyu C. *et al.* The Disease Associated Tau35 Fragment has an Increased Propensity to Aggregate Compared to Full-Length Tau. Front. Mol. Biosci. 8, 779240 (2021).

25. He X. *et al.* Investigation of the structure of full-length tau proteins with coarse-grained and all-atom molecular dynamics simulations. *ACS Chem. Neurosci.* **14**, 209-217 (2023).
26. Zhu H.-L. *et al.* Quantitative characterization of heparin binding to Tau protein: implication for inducer-mediated Tau filament formation, *J. Biol. Chem.* **285**(6), 3592–3599 (2010).
27. Jebarupa B. *et al.*, Effect of altered solution conditions on tau conformational dynamics: plausible implication on order propensity and aggregation. *BBA – Proteins and Proteomics* **1866**, 668-679 (2018).
28. Boyko S. *et al.* Liquid-liquid phase separation of tau protein: The crucial role of electrostatic interactions. *J. Biol. Chem.* **294**(29) 11054-11059 (2019).
29. Hatae J. *et al.* Determination of the appropriate valence of 1,4-piperazinediethanesulfonic acid (PIPES) in physiological pH. *Biol. Pharm. Bull.* **17**(3), 437-439 (1994).
30. Jones J. B. *et al.* Interplay between liquid crystalline and isotropic gels in self-assembled neurofilament networks. *Biophys. J.* **95**, 823-825 (2008).
31. Deek J. *et al.* Neurofilament networks: Salt-responsive hydrogels with sidearm-dependent phase behavior. *Biochim. Biophys. Acta – General Subjects* **1860**, 1560-1569 (2016).
32. Yoon J. *et al.* Small-angle X-ray scattering station 4C2 BL of Pohang accelerator laboratory for advance in Korean polymer science. *Macromolecular Research* **16**(7), 575-585 (2008).
33. Manalastas-Cantos K. *et al.* ATSAS 3.0: expanded functionality and new tools for small-angle scattering data analysis. *J. Appl. Cryst* **54**, 343-355 (2021).
34. Kohn, J. E. *et al.* Random-coil behavior and the dimensions of chemically unfolded proteins. *Proc. Natl Acad. Sci. USA* **101**, 12491–12496 (2004).
35. Schwalbe M. *et al.* Structural impact of Tau phosphorylation at threonine 231. *Structure* **23**, 1448-1458 (2015).
36. Wickramsinghe S. P. *et al.* Polyphosphate initiates tau aggregation through intra- and inter-molecular scaffolding. *Biophys. J.* **117**, 717-728 (2019).

Figures

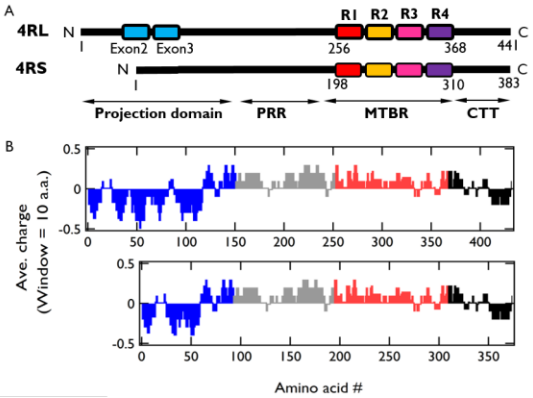

Fig. 1 (a) Human wild-type Tau 4RS and 4RL possess four imperfect repeats (R1, R2, R3, and R4) and differ in the N-terminal region by possessing either zero or two 29-amino-acid regions, thereby generating short (S-) or long (L-) isoforms. The numbers below each isoform refer to the first residue of the isoform, the beginning residues for the repeat region and the C-terminal tail, and the last residue of the isoform. (b) Charge (average over 10 residues) vs. amino acid residue number for 4RS and 4RL Tau. The charge distribution diagram of each isoform shows the cationic and anionic nature of Tau. Tau consists of the projection domain (blue) and proline-rich region (PRR, grey), followed by the microtubule-binding region (MTBR, red) and C-terminal tail (CTT, black).

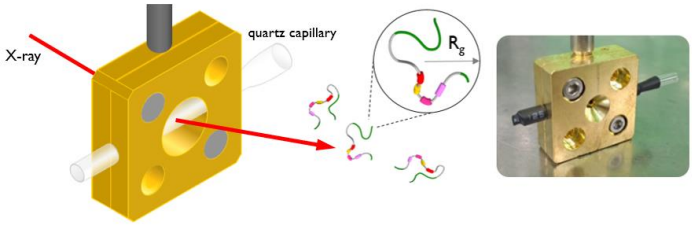

Fig. 2 Schematic illustration of solution X-ray scattering cell measuring the radius of gyration of Tau.

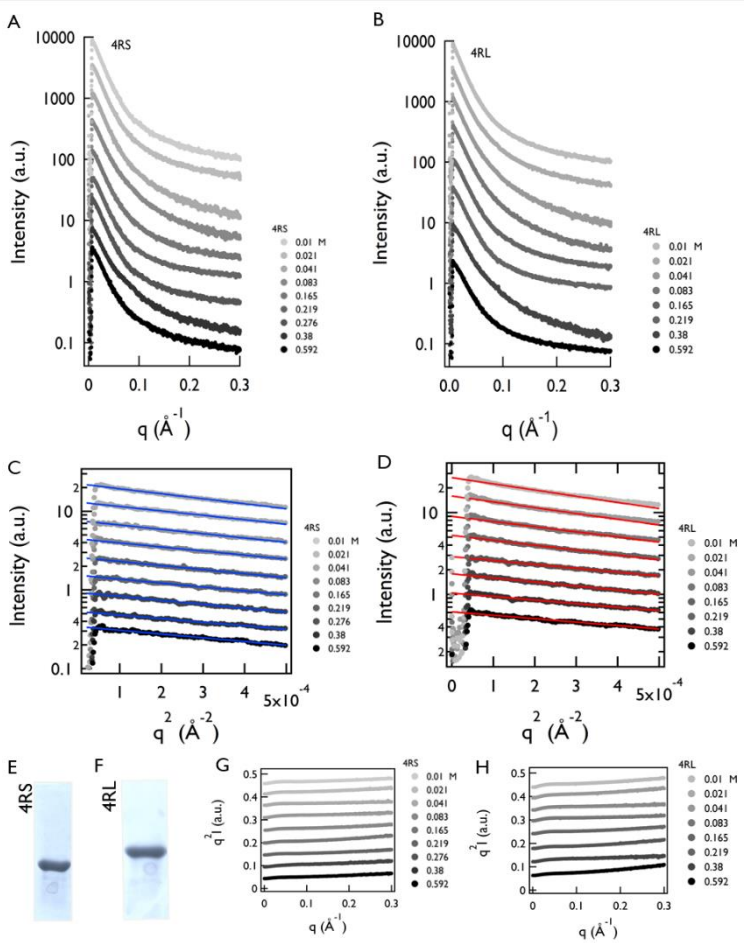

Fig. 3 (a-b) Synchrotron solution X-ray scattering plot of 4RS (a) and 4RL (b) as a function of ionic strength. **(c-d)** Guinier plot (I vs. q^2) for 4RS and 4RL. Colored lines are the fit results of X-ray data to the equation $I = I(0)$ exp ($-q^2R_g^2/3$). **(e-f)** Gel image of purified 4RS (e) and 4RL (f) for X-ray scattering. **(g-h)** Kratky plot (q^2I vs. q) for 4RS and 4RL as a function of ionic strength.

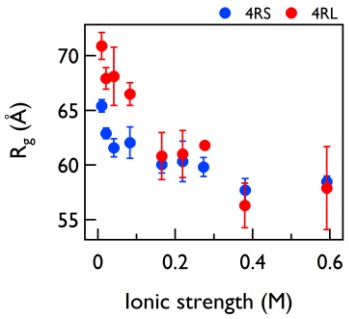

Fig. 4 R_g plot as a function of ionic strength for 4RS and 4RL.

Synchrotron X-ray Study of Intrinsically Disordered and Polyampholytic Tau 4RS and 4RL under Controlled Ionic Strength

Hasaeam Cho[1], Jimin Lee[1], Hanjoon Nho[1], Keunmin Lee[1], Bopil Gim[1], Juncheol Lee[1], Jaehee Lee[1], Kai K. Ewert[2], Youli Li[3], Stuart C. Feinstein[4], Cyrus R. Safinya[2], Kyeong Sik Jin[5,6], Myung Chul Choi[1*]

[1]Department of Bio and Brain Engineering, KAIST, Daejeon 305-701, Korea*
[2]Materials Department, Molecular, Cellular, and Developmental Biology Department, Physics Department, and Biomolecular Science and Engineering Program, University of California, Santa Barbara, California 93106, USA
[3]Materials Research Laboratory, University of California, Santa Barbara, California 93106, USA
[4]Neuroscience Research Institute, Molecular, Cellular, and Developmental Biology Department, and College of Creative Studies Biology, University of California, Santa Barbara, California 93106, USA
[5]Pohang Accelerator Laboratory, POSTECH, Pohang 37673, Korea
[6]Division of Advanced Nuclear Engineering, POSTECH, Pohang 37673, Korea

*Corresponding author. E-mail: mcchoi@kaist.ac.kr

Abstract. Aggregated and hyperphosphorylated tau is one of the pathological hallmarks of Alzheimer's disease. Tau is a polyampholytic and intrinsically disordered protein (IDP). In this paper, we present for the first time experimental results on the ionic strength dependence of the radius of gyration (R_g) of human Tau 4RS and 4RL isoforms. Synchrotron X-ray scattering revealed that 4RS R_g is regulated from 65.4 to 58.4 Å and 4RL R_g is regulated from 70.9 to 57.8 Å by varying ionic strength from 0.01 to 0.59 M. The R_g of 4RL Tau is larger than 4RS at lower ionic strength. This result provides an insight into the ion-responsive nature of intrinsically disordered and polyampholytic Tau, and can be implicated to the further study of Tau-Tau and Tau-tubulin intermolecular structure in ionic environments.

Keywords: Tau, IDP, R_g, X-ray scattering

1 Introduction

The protein Tau is mostly localized in axons of neurons and plays a key role in neuronal development including cell polarity, outgrowth, dendrite pruning, and DNA protection. [1-8] Tau is known as a microtubule-associated protein (MAP). Tau binds to microtubule (MT), regulates tubulin assembly, and stabilizes MTs. [9-12] Aberrant Tau behavior is correlated with numerous neurodegenerative diseases including Alzheimer's,

Pick's, supranuclear palsy, and fronto-temporal dementia with Parkinsonism linked to chromosome 17 (FTDP-17) [13, 14].

Tau is an intrinsically disordered protein (IDP) that lacks a secondary structure in solution. [15, 16] In cells, Tau undergoes liquid-liquid phase separation (LLPS) similar to several IDPs and low-complexity regions in proteins, with high local protein concentration within condensed drops. [17, 18] The Tau structure is often described sequentially from the N- to the C-terminus: human wild-type Tau 4RS and 4RL possess four imperfect repeats (R1, R2, R3, and R4) and differ in the N-terminal region by possessing either zero or two sections of 29 amino acids, thereby generating short (S-) or long (L-) isoforms. Tau is a polyampholyte that contains both positive and negative charges within a single Tau. The MT binding domain is rich in positive charge and the N-terminal tail contains regions of negative charge as well as regions rich in positive charge (**Fig. 1B**). Tau is overall cationic with charge in a range of 5.9 – 16.5 *e* at pH 6.8. [9-12]

This intrinsically disordered and polyampholytic nature makes it difficult to understand the structure and function of Tau. The radius of gyration (R_g) a size parameter (or mass distribution) is defined as the square root of the average squared distance of each scatterer from the particle center. [19] The R_g of 4RL Tau (2N4R or ht40) was measured to be on average 6.5 – 7 nm at room temperature and 5.5 – 7 nm at various temperatures (280 – 333 K). [20-24] Molecular dynamics (MD) simulations gave an R_g of 6.53 nm for 4RL. [25]. For 3RS (0N3R or ht23) and 3RL (2N3R) Tau, R_g values were measured to be 5.3 nm and 6.33 nm, respectively. [20, 21, 24]

Tau is abundant in charged residues and the ionic strength of its solution can be attributed to the conformational transition, which minimizes or maximizes the electrostatic interaction. [26, 27] Human 4RL Tau fibrillation into paired helical filaments (PHFs) found in the brains of AD patients can be induced by heparin, and decreases with increasing ionic strength. [26, 27] In condensed LLPS drops, PHF formation is promoted in the presence of heparin, and is dependent on ionic strength: PHFs were not observed at NaCl concentrations of 200 mM and above. In the absence of heparin, however, Tau MTBRs merely form PHF despite ionic strength changes in 0-300 mM NaCl. [17] Tau LLPS formation is sensitive to the salt concentration, being enhanced at low salt concentrations and inhibited at high concentrations by adding more than 200 mM NaCl or KCl. [18, 28] X-ray scattering can be employed to quantitatively characterize the overall structure and structural transitions of partially or completely unfolded proteins and metastable objects. [21] However, the overall size of Tau protein under ionic strength regulation is not yet understood, and remains to be elucidated.

In this paper, we have used synchrotron X-ray scattering to investigate the structure (i.e. R_g) of human Tau 4RS and 4RL isoforms under controlled ionic strength. We show that the R_g value of both 4RS and 4RL Tau are regulated with varying ionic strength in the range of 0.01 – 0.59 M.

2 Materials, Method, and Results

2.1 Tau protein preparation

Tau is expressed in BL21 (DE3) competent cells. After incubation in LB and auto-induction media (10 g of tryptone, 5 g of yeast extract, 0.5 g of dextrose, 2 g of α-D-lactose and 5 mL of glycerol per liter of 25 mM Na_2HPO_4, 25 mM KH_2PO_4, 50 mM NH_4Cl, 5 mM Na_2SO_4, and 4 mM $MgSO_4$ in DI water) for 24 h, cells were collected via centrifugation, and were re-suspended in BRB80 (80 mM PIPES/NaOH at pH 6.8, 1 mM EGTA, 1 mM $MgSO_4$), [9-12] lysed via sonication, and then subsequently boiled and centrifuged again. The supernatant was run through a phosphocellulose (P11 Whatman) anionic exchange column, with Tau binding to the phosphocellulose, and eluted with increasing concentration of NaCl in BRB80. Fractions with Tau were buffer-exchanged into pure BRB80 via Amicon Ultra-15 Centrifugal Units (Millipore). Tau was loaded into a HiTrap hydrophobic interaction chromatography column (GE), and eluted with decreasing the concentration of $(NH_4)_2SO_4$ in BRB80. Tau was concentrated and the buffer was exchanged with pure BRB80 through successive centrifugation cycles using Amicon Centrifugal Units. The concentration of Tau stock was determined by SDS-PAGE comparison with a Tau mass standard (originally measured via amino acid analysis).

2.2 Control in ionic strength

For BRB80 buffer, [Pipes] = 80 mM, $[Pipes^{2-}] = [Pipes^{-}] \approx 40$ mM and $[Na^{+}] = [NaOH] = [Pipes^{-}] + 2 \times [Pipes^{2-}] \approx 120$ mM, at pH ≈ 6.8 due to pKa_1=3.3 and pKa_2 = 6.85 at 20 °C. [29] The ionic strength, $\mu = \Sigma\, \rho_i z_i^2 / 2 = ([Pipes^{2-}] \times (-2)^2 + [Pipes^{-}] \times (-1)^2 + [Na^{+}] \times (+1)^2) / 2 = ([0.04] \times (-2)^2 + [0.04] \times (-1)^2 + [0.12] \times (+1)^2) / 2 = 0.16$ M. (With $[MgCl_2]$ = 1 mM, and [EGTA] = 1 mM, μ ≈ 0.165 M, while EGTA is a chelator of Mg^{2+} ion.) To vary the ionic strengths at constant pH: PEM80 buffer was diluted by adding deionized water, thus μ = 0.01 – 0.165 M. KCl was added to PEM80 buffer for μ = 0.165 – 0.59 M. [9, 30-31]

2.3 Synchrotron X-ray scattering.

Synchrotron X-ray scattering was carried out at the Pohang Accelerator Laboratory (PAL) beam-line 4C at 10 keV. [32] Scattering data were collected with a Rayonix 2D SX165 detector. Sample-to-detector distance was set to 4 m for SAXS or 4 m and 2 m for merging of SAXS and WAXS and calibrated with a silver behenate reference sample. The images were azimuthally averaged to obtain scattering intensity versus momentum transfer q. Fig. 2 shows a customized solution X-ray scattering cell: it is made of brass. A 1.5 mm quartz capillary was mounted in the cell. The temperature was controlled using an oil circulator (FP5-HE and H10, Julabo). Our scattering experiment was carried out at 20 °C. As a control sample, bovine serum albumin (BSA) was loaded and data was compared with the known scattering patterns. Buffer data was previously collected for 10 sec as the background. For each scattering sample, data was collected for 10 sec which is the time for the Tau sample to be safe from radiation damage (see **Fig. S2**. Six rounds of data collection were averaged, and background buffer data was subtracted with PRIMUS. [33] The forward scattering *I(0)* and the radius of gyration

R_g were evaluated using the Guinier approximation, which states that the intensity can be represented as $I(q) = I(0)$ exp $[-(q^2R_g^2)/3]$ at small angles of $q < 1.3/R_g$. [19-20]

Tau samples for X-ray scattering were concentrated with an Amicon Ultra-0.5 device (Millipore) at 13170 g (RCF) for 10 min at room temperature. The final Tau concentration was 4 – 8 mg/mL. At least 25 µL of the sample was loaded in a 1.5 mm quartz capillary that had been washed with ethanol and deionized water.

Our X-ray samples used for the determination of R_g exhibits a completely linear Guinier plot (**Fig. S1**) indicating non-aggregated ones, which is distinguished from the aggregated sample of a nonlinear X-ray scattering profile at the small angle (q). Consistently, the gel permeation chromatography (GPC) result shown in **Fig. S3** has a single peak for 4RS Tau and no sign of aggregation.

Fig. 3(C-D) shows the azimuthally-averaged synchrotron X-ray scattering data of 4RS and 4RL with varying ionic strength µ = 0.01 – 0.59. To quantitatively assess the effect of ionic strength on the R_g of Tau, the Guinier plots of scattering intensity vs. q^2 are shown in **Fig. 3(E-F)**, where the y-axis is in the log scale. Note that all the scattering data in the Guinier regime are linear, indicating that the Tau samples were not aggregated. **Fig. 3(G-H)** shows Kratky plots of $q^2I(q)$ *vs* q, which show featureless curves without apparent peaks which is typical for unfolded proteins. [20]

The fit of the X-ray data to the equation $I = I(0)\exp(-q^2R_g^2/3)$ gives the R_g of Tau. **Fig. 4** shows that the R_g of both 4RS and 4RL increases as the ionic strength (µ) decreases. With decreasing µ from 0.59 to 0.01 M, the R_g of 4RS Tau increases from 58.5 to 65.4 Å (12.0 % increase); R_g increases from 57.9 to 70.9 Å (22.7 % increase) for 4RL Tau. We note that the main change in R_g occurs at low ionic strength: For example, at $\mu \leq 0.165$, 76.4 % of the change in R_g occurs for 4RS and 77.0 % of the change for 4RL. The change in R_g then mostly saturates at $\mu > 0.165$. In comparison between 4RS and 4RL, 4RL is in general larger than 4RS. Particularly at µ = 0.01 – 0.083, the difference in R_g between 4RS and 4RL is significantly large to be 5.37 ± 0.87 Å, but $\mu \geq 0.165$, the R_g of 4RL Tau is slightly larger (µ = 0.165 – 0.273) and smaller (µ = 0.381 – 0.592) than 4RS.

The R_g of unstructured protein is found to fit with Flory equation [34] $R_g = (1.927)N^{0.588}$ Å: R_g = 69.15 Å for 4RL (N_{4RL} = 441) and R_g = 63.65 Å for 4RS (N_{4RS} = 383). Our X-ray scattering data for the ionic strength µ = 0.083 (Debye length is $1/\kappa$ = 10.59 Å) which are R_g = 62.05 Å for 4RS and 66.48 Å for 4RL, are comparable to the theoretical estimation. On the other hand, at higher ionic strength $\mu \geq 0.165$ M, the smaller R_g with monotonically decreasing and isoform-independent manner might be due to the suppression of electrostatic interaction, thus the predominantly hydrophobic inter-residue attraction of single Tau. However, the structure and interaction of Tau isoforms for the low ionic regime have not been well understood yet, which needs to be elucidated.

3 Conclusion

We present a synchrotron solution X-ray scattering study to quantitatively measure the radius of gyration R_g of human Tau particularly the 4RS and 4RL isoforms in an ionic environment. Upon varying ionic strength from 0.01 – 0.59 M, R_g of Tau was

regulated: for 4RS, R_g increased from 58.4 to 65.4 Å; for 4RL R_g increased from 57.8 to 70.9 Å. Thus, 4RL Tau R_g is larger in a lower ionic strength environment than 4RS. This is the first experimental demonstration that the ionic strength dependence of the radius of gyration of full-length human Tau has been measured.

This paper provides insight into the regulation of the ionic environment-responsive nature of the intrinsically disordered and polyampholytic protein Tau. Changes in the charge environment such as a fluctuation in ionic strength or charge modification (e.g. post-translational modification including phosphorylation, etc.) might have significant effects on the structure and interaction of Tau and microtubules. [26-27, 35-36] For example, the expanded Tau molecules can be reactive to bind with another Tau or with tubulin in the neuronal cell. This highly interactive environment of Tau is analogously found in the confined space of Tau LLPS, where Tau-induced microtubule growth is known to occur. [18]

This result can be implicated to the further study of Tau-Tau and Tau-tubulin intermolecular structure regulated by the ionic environment. Molecular dynamics simulation study can determine the R_g of ionically regulated polyampholytic Tau.

Acknowledgments. This work was supported by KAIST KC30-N11230021, NRF-2021R1A6A3A13046235, KHID/KDRC-MOHW/MIST-HU23C0094, KBSI-MOE-2021R1A6C103B422 and NRF-MIST-2020M3A7B6026565. K.S.J. was supported by NRF- 2020R1F1A1054849. C.R.S., Y.L., and K.K.E. were supported by the US DOE, Office of Basic Energy Sciences, Division of Materials Sciences and Engineering under award number DE-FG02-06ER46314 (self- and directed assembly in charged biomolecular materials). Partial support was further provided to C.R.S. by the US NSF under award number DMR-1807327 (for protein phase behavior studies). S.C.F. was supported by a grant from UCSB Academic Senate.

Author contributions. The experiments were conducted by J.L., H.C., J.L., J.L., and K.J. The data were analyzed and discussed by J.L., H.C., C.R.S., Y.L., K.K.E, S.C.F., H.N., K.L., B.G., and M.C.C. The manuscript was written by H.C. and M.C.C. and reviewed by all authors.

Data availability. The data supporting this study are available from the corresponding author on reasonable request.

References

1. Scholz T. *et al.* Transport and diffusion of tau protein in neurons. *Cell. Mol. Life Sci.* **71**, 3139-3150 (2014).
2. Drubin D.G. *et al.* Nerve growth factor-induced neurite outgrowth in PC12 cells involves the coordinate induction of microtubule assembly and assembly-promoting factors. *J Cell Biol* **101**, 1799 –1807 (1985).
3. Esmaeli-Azad B. *et al.* Sense and antisense transfection analysis of tau function—tau influences net microtubule assembly, neurite outgrowth, and neuritic stability. *J Cell Sci* **107**, 869–879 (1994).

4. Ferreira A. *et al.* Microtubule formation and neurite growth in cerebellar macroneurons which develop in vitro: evidence for the involvement of the microtubule-associated proteins, MAP-1a, HMW-MAP2, and Tau. *Brain Res Dev Brain Res* **49**, 215–228 (1989).
5. Kempf M. *et al.* Tau binds to the distal axon early in development of polarity in a microtubule- and microfilament-dependent manner. *J. Neurosci.* **16**(18), 5583–5592 5591 (1996).
6. Herzmann S. *et al.* PAR-1 promotes microtubule breakdown during dendrite pruning in Drosophila. *EMBO J.* **36**, 1981–1991 (2017).
7. Rumpf S. *et al.* Functions of microtubule disassembly during neurite pruning. *Trends in Cell Biology* **29**(4), 291-297 (2019).
8. Sultan A. *et al.* Nuclear tau, a key player in neuronal DNA protection. *J. Biol. Chem.* **286**(6), 4566-4575 (2011).
9. Choi M. C. *et al.* Human microtubule-associated-protein tau regulates the number of protofilaments in microtubules: a synchrotron X-ray scattering study. *Biophys. J.* **97**, 519–527 (2009).
10. Chung P. J. *et al.* Direct force measurements reveal protein Tau confers short-range attractions and isoform-dependent steric stabilization to microtubules. *Proc. Natl Acad. Sci. USA* **112**, E6416–E6425 (2015).
11. Chung P. J. *et al.* Tau mediates microtubule bundle architectures mimicking fascicles of microtubules found in the axon initial segment. *Nat. Commun.* **7**, 12278-12286 (2016).
12. Choi M. C. *et al.* Paclitaxel suppresses Tau-mediated microtubule bundling in a concentration-dependent manner. *Biochimica et Biophysica Acta (BBA) – General Subjects* **1861**(1A), 3456-3463 (2017).
13. Kosik, K. S. *et al.* Microtubule-associated protein tau (tau) is a major antigenic component of paired helical filaments in Alzheimer disease. *Proc. Natl Acad. Sci. USA* **83**, 4044–4048 (1986).
14. Hutton, M. *et al.* Association of missense and 5'-splice-site mutations in tau with the inherited dementia FTDP-17. *Nature* **393**, 702–705 (1998).
15. Jeganathan S. *et al.* The natively unfolded character of tau and its aggregation to Alzheimer-like paired helical filaments. *Biochemistry* **47**, 10526–10539 (2008).
16. Skrabana R. *et al.* Intrinsically disordered proteins in the neurodegenerative processes: formation of tau protein paired helical filaments and their analysis. *Cellular and Molecular Neurobiology* **26**, 1083–1095 (2006).
17. Ambadipudi S. *et al.* Liquid-liquid phase separation of the microtubule-binding repeats of the Alzheimer-related protein Tau. *Nat Commun.* **8**, 275-287 (2017).
18. Hernández-Vega A. *et al.* Local nucleation of microtubule bundles through tubulin concentration into a condensed tau phase. *Cell Reports* **20**, 2304-2312 (2017).
19. Putnam C. D. *et al.* X-ray solution scattering (SAXS) combined with crystallography and computation: defining accurate macromolecular structures, conformations and assemblies in solution. *Quarterly Reviews of Biophysics* **40**(3), 191-285 (2007).
20. Mylonas E. *et al.* Domain conformation of tau protein studied by solution small-angle X-ray scattering. *Biochemistry* **47**, 10345–10353 (2008).
21. Shkumatov A. V. *et al.* Structural Memory of Natively Unfolded Tau Protein Detected by Small-Angle X-ray Scattering. Proteins 79, 2122−2131 (2011).
22. Bianconi A. *et al.* Temperature and solvent dependence of the dynamical landscape of tau protein conformations. *J Biol Phys* **38**, 169-179 (2012)
23. Battisti A. *et al.* Thermal compaction of the intrinsically disordered protein tau: entropic, structural, and hydrophobic factors. *Phys. Chem. Chem. Phys.* **19**, 8435 (2017).
24. Lyu C. *et al.* The Disease Associated Tau35 Fragment has an Increased Propensity to Aggregate Compared to Full-Length Tau. Front. Mol. Biosci. 8, 779240 (2021).

25. He X. *et al.* Investigation of the structure of full-length tau proteins with coarse-grained and all-atom molecular dynamics simulations. *ACS Chem. Neurosci.* **14**, 209-217 (2023).
26. Zhu H.-L. *et al.* Quantitative characterization of heparin binding to Tau protein: implication for inducer-mediated Tau filament formation, *J. Biol. Chem.* **285**(6), 3592–3599 (2010).
27. Jebarupa B. *et al.*, Effect of altered solution conditions on tau conformational dynamics: plausible implication on order propensity and aggregation. *BBA – Proteins and Proteomics* **1866**, 668-679 (2018).
28. Boyko S. *et al.* Liquid-liquid phase separation of tau protein: The crucial role of electrostatic interactions. *J. Biol. Chem.* **294**(29) 11054-11059 (2019).
29. Hatae J. *et al.* Determination of the appropriate valence of 1,4-piperazinediethanesulfonic acid (PIPES) in physiological pH. *Biol. Pharm. Bull.* **17**(3), 437-439 (1994).
30. Jones J. B. *et al.* Interplay between liquid crystalline and isotropic gels in self-assembled neurofilament networks. *Biophys. J.* **95**, 823-825 (2008).
31. Deek J. *et al.* Neurofilament networks: Salt-responsive hydrogels with sidearm-dependent phase behavior. *Biochim. Biophys. Acta – General Subjects* **1860**, 1560-1569 (2016).
32. Yoon J. *et al.* Small-angle X-ray scattering station 4C2 BL of Pohang accelerator laboratory for advance in Korean polymer science. *Macromolecular Research* **16**(7), 575-585 (2008).
33. Manalastas-Cantos K. *et al.* ATSAS 3.0: expanded functionality and new tools for small-angle scattering data analysis. *J. Appl. Cryst* **54**, 343-355 (2021).
34. Kohn, J. E. *et al.* Random-coil behavior and the dimensions of chemically unfolded proteins. *Proc. Natl Acad. Sci. USA* **101**, 12491–12496 (2004).
35. Schwalbe M. *et al.* Structural impact of Tau phosphorylation at threonine 231. *Structure* **23**, 1448-1458 (2015).
36. Wickramsinghe S. P. *et al.* Polyphosphate initiates tau aggregation through intra- and inter-molecular scaffolding. *Biophys. J.* **117**, 717-728 (2019).

Figures

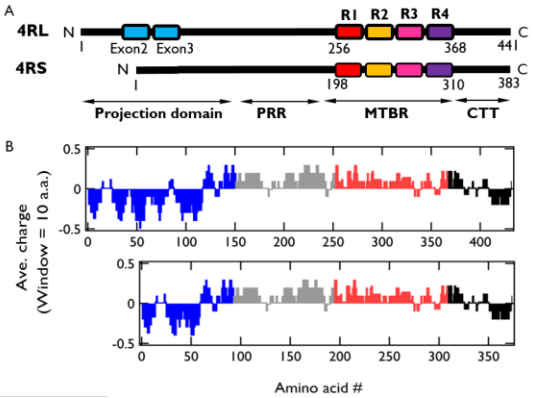

Fig. 1 (a) Human wild-type Tau 4RS and 4RL possess four imperfect repeats (R1, R2, R3, and R4) and differ in the N-terminal region by possessing either zero or two 29-amino-acid regions, thereby generating short (S-) or long (L-) isoforms. The numbers below each isoform refer to the first residue of the isoform, the beginning residues for the repeat region and the C-terminal tail, and the last residue of the isoform. (b) Charge (average over 10 residues) vs. amino acid residue number for 4RS and 4RL Tau. The charge distribution diagram of each isoform shows the cationic and anionic nature of Tau. Tau consists of the projection domain (blue) and proline-rich region (PRR, grey), followed by the microtubule-binding region (MTBR, red) and C-terminal tail (CTT, black).

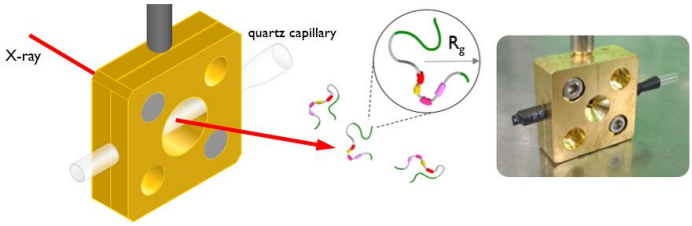

Fig. 2 Schematic illustration of solution X-ray scattering cell measuring the radius of gyration of Tau.

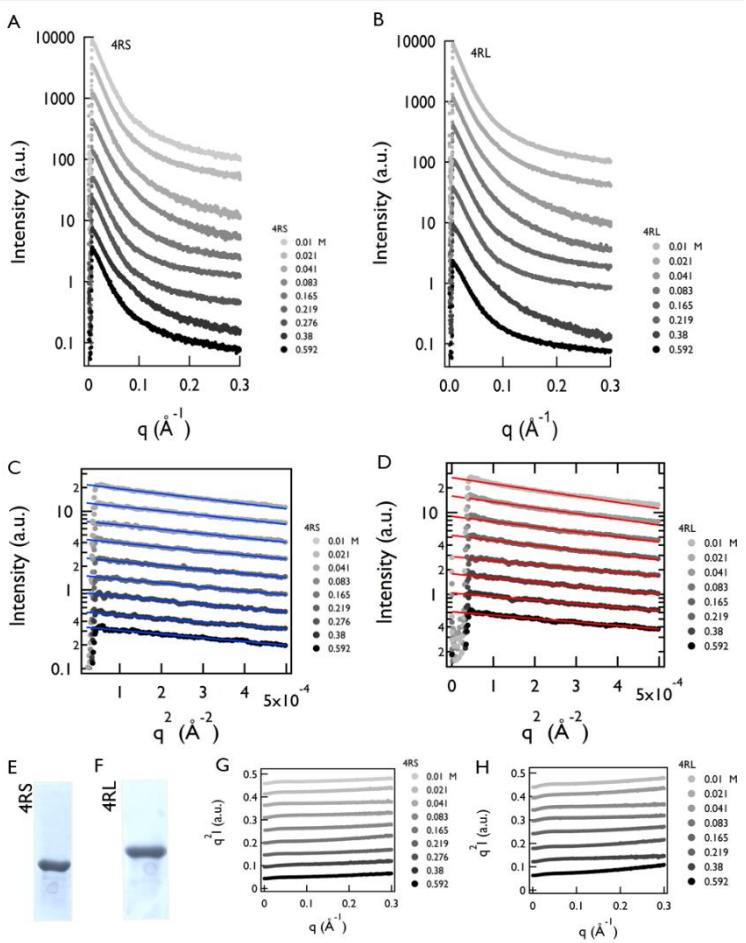

Fig. 3 (a-b) Synchrotron solution X-ray scattering plot of 4RS (a) and 4RL (b) as a function of ionic strength. **(c-d)** Guinier plot (I vs. q^2) for 4RS and 4RL. Colored lines are the fit results of X-ray data to the equation $I = I(0)$ exp ($-q^2R_g^2/3$). **(e-f)** Gel image of purified 4RS (e) and 4RL (f) for X-ray scattering. **(g-h)** Kratky plot (q^2I vs. q) for 4RS and 4RL as a function of ionic strength.

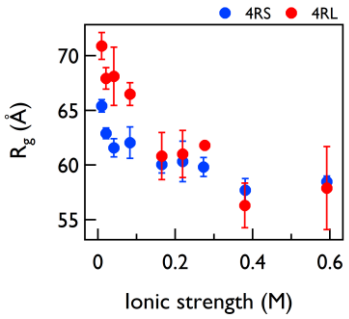

Fig. 4 R_g plot as a function of ionic strength for 4RS and 4RL.

Graphical Abstract
For

Synchrotron X-ray Study of Intrinsically Disordered and Polyampholytic Tau 4RS and 4RL under Controlled Ionic Strength

Hasaeam Cho[1], Jimin Lee[1], Hanjoon Nho[1], Keunmin Lee[1], Bopil Gim[1], Juncheol Lee[1], Jaehee Lee[1], Kai K. Ewert[2], Youli Li[3], Stuart C. Feinstein[4], Cyrus R. Safinya[2], Kyeong Sik Jin[5,6], Myung Chul Choi[1]

[1]*Department of Bio and Brain Engineering, KAIST, Daejeon 305-701, Korea*
[2]*Materials Department, Molecular, Cellular, and Developmental Biology Department, Physics Department, and Biomolecular Science and Engineering Program, University of California, Santa Barbara, California 93106, USA*
[3]*Materials Research Laboratory, University of California, Santa Barbara, California 93106, USA*
[4]*Neuroscience Research Institute, Molecular, Cellular, and Developmental Biology Department, and College of Creative Studies Biology, University of California, Santa Barbara, California 93106, USA*
[5]*Pohang Accelerator Laboratory, POSTECH, Pohang 37673, Korea*
[6]*Division of Advanced Nuclear Engineering, POSTECH, Pohang 37673, Korea*

*Corresponding author. E-mail: mcchoi@kaist.ac.kr

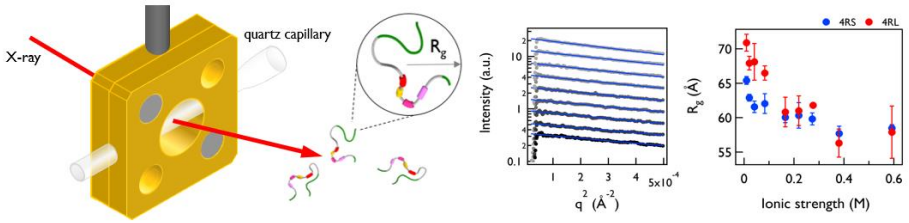
X-ray
quartz capillary
R_g
Intensity (a.u.)
q^2 ($Å^{-2}$)
5x10^{-4}
4RS
4RL
R_g (Å)
Ionic strength (M)

Answers to Reviewer's Comments

for

EPJE-D-23-00143

Reviewer 1

[Comment 1] The graphical items of Fig.3 are quite small, the display of the Guinier fits would benefit from enlarging the Figure. The labels of the different curves would then also be better visible.

[Answer 1] We thank the reviewer's comment. We have revised the Fig. 3.

[Comment 2] The choice of buffer and of changing ionic strength with KCl instead von NaCl could be motivated in the introduction, including references.

[Answer 2] For reviewer's comment on "the choice of buffer": In section 2.1 (line 7), where we describe Tau buffer BRB80, the reference [9-12] is addressed now. Using BRB80 for Tau study is reasonable because BRB80 is the co-buffer for both of Tau and microtubule.

For reviewer's comment on "changing ionic strength with KCl": Inside neuron, KCl concentration is higher than NaCl. The K+ ion is known to have a higher probability of being closer to the N-terminal region of Tau than Na+. (T. Gastro et al., Biomolecules, 9, 116 (2019)) In section 1. introduction (line 34), we addressed "Tau LLPS formation is sensitive to the salt concentration, being enhanced at low salt concentrations and inhibited at high concentrations by adding more than 200 mM NaCl or KCl. [18, 28]" We also addressed in section 2.2 (line 27) the reference papers [9, 30-31] that have used KCl for changing the ionic regulation.

[Comment 3] The data acquisition of 10 seconds seems quite long; more details on primary intensity, dose and possible radiation damage would be valuable in view of comparing the study to other protein SAXS studies.

[Answer 3] The **Fig. R1** shows the synchrotron X-ray scattering intensity vs. q^2 for the several data acquisition times. The data with 5 sec and 10 sec acquisition times show a linear scattering profiles, whereas 15 sec data exhibit non-linear profiles in low q. We revised the manuscript by adding the sentence "…10 seconds which is the time for Tau sample to be safe from the radiation damage". We included **Fig. R1** in Supplementary Information, as **Fig. S2**.

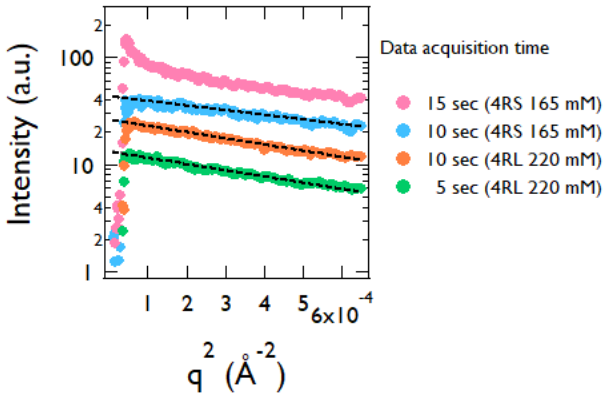

Fig. R1 Synchrotron X-ray scattering intensity vs. q^2 for the several data acquisition times.

Reviewer 2

[Comment 1] I strongly suggest the deposition of the data to a public database, such as SASBDB, and addition of the accession numbers to the manuscript.

> **[Answer 1]** We agree with the reviewer's suggestion. We would deposit the data to public database, which however could be after when we report another paper on the structure of Tau by ionic regulation that we are in preparation now. We will appreciate for reviewer's understanding on our current situation.

[Comment 2] No explanation is given for the difference in the ionic dependence of the R_g between 4RL and 4RS. It needs to be further discussed in the Conclusion section and the authors should try to provide a hypothesis for this difference.

> **[Answer 2]** We thank the reviewer's comment. Flory equation predicts the R_g of random coil conformation as $R_g = (0.1927\ Å)\ N^{0.588}$ nm (Kohn, J. E. *et al.* PNAS **101**, 12491–12496 (2004)). For intrinsically disordered protein Tau, R_g = 63.65 Å (N = 441 for 4RS), and 69.15 Å (N = 383 for 4RL). From our X-ray scattering measurements, R_g = 62.05 Å for 4RS and 66.48 Å for 4RL for the ionic strength μ = 0.083 (Debye screening length is $1/\kappa$ = 10.59 Å), which is comparable to the theoretical prediction. On the other hand, at higher ionic strength $\mu \geq 0.165$ M, R_g is monotonically decreasing in the range of 56.3 – 61.01 Å and comparable between 4RS and 4RL. It can be explained by the interplay between electrostatic and hydrophobic interactions: with increasing ionic strength the electrostatic interaction is suppressed, thus hydrophobic inter-residue attraction of single Tau can induce smaller R_g. However, to be honest, we have not well explained it yet our R_g results of low ionic strength regime in terms of structure and interaction, which definitely need be elucidated. Indeed, we are under investigation of the form factor of Tau isoforms in ionic strength dependent manner. We addressed it in the section 2.3 (line 26 – 40) of the manuscript (colored in blue). Also, our manuscript had addressed in the last sentence of the conclusion "Also, the numerical estimation and molecular dynamics simulation studies can determine the form factor of ionically regulated Tau isoforms."

[Comment 3] It would be useful to add a few specific comments of the biological relevance of the results in the Conclusion section, i.e. what is the relevant ionic strength inside the cells/LLPS regions, how ionic strength changes could affect the function or pathogenicity of Tau etc.

> **[Answer 3]** We thank the reviewer's comment. It is not well understood how much the ionic strength is fluctuated inside the cell and inside LLPS. We do not attempt to claim that the ion fluctuation in the cell reaches to such low ionic strength level to which our paper covers. Our paper rather delivers the message that the low ionic environment, where the electrostatic interaction between residues-residue or between Tau-Tau is amplified, is relevant (corresponds) to the strong interaction regime of Tau molecules in LLPS where the density of Tau is significantly high. We note that the formation of Tau LLPS is sensitive to (i) the salt concentration (induced at low salt) and (ii) Tau density (induced at high Tau). [17-18, 28]
>
> Our manuscript had addressed in the conclusion "For example, the expanded Tau molecules can be reactive to the binding with another Tau or tubulin in the neuronal cell. This highly interactive environment of Tau is analogously found in the confined space of Tau LLPS, where Tau-induced microtubule growth is known to occur."

[Comment 4] Although the manuscript is not difficult to follow in general, it would benefit from copyediting to improve the language.

> **[Answer 4]** We thank the reviewer's suggestion. We did revise our manuscript via copyediting.

[Comment 5] Specific comments

1. In the abstract p.1-l.22 please revise the following sentence: "Tau is one of the pathogens of Alzheimer's disease." Tau is not a pathogen per se. It is a protein with an important physiological role that is also involved in Alzheimer's disease pathogenicity.
2. In the abstract p.1-l.27: "The R_g of 4RL Tau is more extended than 4RS at lower ionic strength." Since Rg is a scalar quantity, "more extended" should be replaced with "larger".
3. P.2-l.6: "In the body" is too general. LLPS of Tau happens inside of cells.
4. R_g should always be with a subscript.
5. P.4-l.1: Superscripts and subscripts should be used in the equation.
6. P.4-l.14: "The fit of the X-ray data to the equation $S = I\,0 \exp(-q^2R_g2/3)$ gives Tau's R_g." S should be I(q). Also be consistent in the way you refer to I(0). Sometimes it is I(0), other times it is I0.
7. P.4-l.39: "Thus, 4RL Tau R_g is more extended in a lower ionic strength environment than 4RL". R_g should be removed and the second 4RL should be, I believe, 4RS.
8. P.5-l.21: "conducted the experiments" should be removed.
9. Figure 1 legend: "either zero or two 29 amino acids" should be "either zero or two 29-amino-acid regions".
10. SI Fig. 1: It is not clear why one sample is aggregated and the other not. Also, the last paragraph of section 2.3 (p.4) should be moved to the beginning of the section, before the Rg analysis.

[Answer 5] We thank the reviewer's comments.

1. We did correct the sentence, which was marked in blue color.
2. We did correct it (colored in blue).
3. We did change it into "cells".
4. We did check this out.
5. We did check this out.
6. We did correct typos.
7. We did correct it.
8. We did remove it.
9. We did change it.
10. The aggregated samples, which were stored at 4 ^{o}C and at high concentration of 6 mg/mL for over 30 months, have been first checked by SDS PAGE and then followed by X-ray experiments. And, as the reviewer commented, we did move the paragraph ahead of describing Fig. 3